Pulsed laser induced atomic layer etching of silicon

Cite as: J. Vac. Sci. Technol. A 41, 022602 (2023); https://doi.org/10.1116/6.0002399 Submitted: 06 December 2022 • Accepted: 01 February 2023 • Published Online: 28 February 2023

🔟 Matthew Eliceiri, 🔟 Yoonsoo Rho, 匝 Runxuan Li, et al.













Pulsed laser induced atomic layer etching of silicon

Cite as: J. Vac. Sci. Technol. A 41, 022602 (2023); doi: 10.1116/6.0002399 Submitted: 6 December 2022 · Accepted: 1 February 2023 · Published Online: 28 February 2023









Matthew Eliceiri, 1 📵 Yoonsoo Rho, 1,2 📵 Runxuan Li, 1 📵 and Costas P. Grigoropoulos 1, a 📵





Laser Thermal Laboratory, Department of Mechanical Engineering, University of California, Berkeley California, 94720

Note: This paper is part of the 2023 Special Topic Collection on Atomic Layer Etching (ALE).

a)Electronic mail: cgrigoro@berkeley.edu

ABSTRACT

We demonstrate the laser mediated atomic layer etching (ALEt) of silicon. Using a nanosecond pulsed 266 nm laser focused loosely over and in a parallel configuration to the surface of the silicon, we dissociate Cl2 gas to induce chlorination. Then, we use pulsed picosecond irradiation to remove the chlorinated layer. Subsequently, we perform continuous wave (CW) laser annealing to eliminate amorphization caused by the picosecond laser etching. Based on atomic force microscopy (AFM) and X-ray photoelectron spectroscopy (XPS), we observed strong evidence of chlorination and digital etching at 0.85 nm etching per cycle with good uniformity.

Published under an exclusive license by the AVS. https://doi.org/10.1116/6.0002399

I. INTRODUCTION

The ALEt of silicon has become a topic of significant interest in recent years due to the ever-shrinking lateral critical feature sizes of lithographic patterning. Very soon, the critical dimension of state-of-the-art consumer electronics will approach several atoms. To keep up with this resolution, the etching process must be equally well controlled, with the goal of etching in the range of 1-3 atomic layers at a time. Additionally, advanced etching processes should possess self-limiting characteristics to ensure uniformity in material removal. The most advantageous version of this selflimiting behavior is referred to as digital etching, where the etch rate exhibits a sharp plateau, after which no further etching is observed with increasing etchant dose. Further attributes of interest for such processes are dry processing, iteration speed, iterative repeatability, and substrate damage avoidance.

The current dominant method of performing ALEt in silicon is reacting Cl2 gas with the silicon surface, forming a surface layer of SiCl. Two main methods have so far been explored to perform the chlorination: thermal chlorination and plasma chlorination. To perform thermal chlorination, the Si substrate must be heated and exposed to Cl₂ gas, at which point the gas will spontaneously react with the surface. Increasing the temperature of the wafer can increase the speed of the reaction, but the temperature must be

maintained well below 650 °C to avoid spontaneous etching.2 Thermal chlorination has been shown to be able to saturate the surface in time periods as short as 8-40 s,³ however this time is still significant. Plasma chlorination is orders of magnitude faster, saturating a surface in as little as 1 s.4 Plasma chlorination has most notably been performed by the use of an inductively coupled plasma. This bonding weakens the adjacent internal Si-Si bonds.⁵ Next, reactive ions are bombarded on the surface where they will selectively remove the weakened bonds. Typically, Ar⁺ ions are used to perform the bombardment and etch the silicon layer^{3,6-8} This process as a whole has been extensively studied both experimentally^{3,5,8-17} and via molecular dynamics. ^{18,19} While plasma etching is promising, unwanted "background" chemical etching and physical sputtering by energetic ions may compromise the quality.

Here, we present a method for the ALEt of silicon by using a two-step pulsed laser chemical assisted etching process. We replaced the high energy inductively coupled plasma source with a nanosecond pulsed UV laser to dissociate the Cl2 molecule and introduce Cl radicals onto the Si surface. The use of a laser presents significant upsides for the industrial application of silicon ALEt because it provides a more controllable and practically easier process compared to plasma chlorination while maintaining short saturation time. In addition, the laser dissociated radicals possess low momentum energy, reducing damage to the samples due to the

²Physical & Life Sciences and NIF & Photon Sciences, Lawrence Livermore National Laboratory, Livermore, California 94550

absence of external driving forces such as an electric field.²⁰ The use of pulsed laser irradiation to finally etch the layer of silicon is also advantageous compared to Argon ion bombardment because of the short time required to produce such pulses and the relatively low vacuum requirements. Furthermore, it offers spatial selectivity, avoiding damage to adjacent structures. Several downsides exist to using laser etching. Optical viewports must be added to couple the laser inside the vacuum chamber. Additionally, direct laser writing is diffraction limited in lateral resolution unless more involved near field optics or mask projection systems are used. Careful design of the optical system and choice of laser pulse energy and repetition rate must be performed as well to reduce processing times. Overall, however, the flexibility of the optical methods presented can offer significant upsides for device fabrication. We note that ALEt using laser irradiation has been investigated for the GaAs and AlGaAs material systems using chlorination and nanosecond pulsed excimer lasers. 6,21,22 Additionally, laser assisted chemical etching has been demonstrated in silicon, but strict self-limiting requirements have not been met.^{23–25} The demonstration of self-limited ALEt by use of laser etching in silicon is the key contribution of the current work.

II. TWO LASER BEAM ASSISTED ETCHING

We began with a heavily Boron doped silicon chip and performed an HF dip to remove the surface oxide layer, and immediately inserted the chip into the vacuum chamber. After lowering the pressure of the chamber to below 5 m Torr via a mechanical pump, we flowed 1% Cl₂ gas in He at a pressure of 200 Torr. Once the chamber attained the setpoint pressure, a 266 nm laser with 5 ns pulse width (Continuum Surelite I-10) was loosely focused over the target with the central focus at 1 mm above the surface of the Si chip having to a beam diameter of $50 \,\mu m$ and a focal length of ~8 mm, propagating parallel to the surface [Fig. 1(a)(i)]. The laser was allowed to emit 35 mJ energy pulses at 10 Hz. After 3 min, the laser was turned off and pressure was reduced to below 5 m Torr. We then focused a 355 nm laser with 4 ps pulses (Passat Compiler) to a $5 \mu m$ beam waist directly on the Si surface [Fig. 1(a)(ii)]. The applied fluence range was 0.1–0.19 J/cm². This picosecond pulse imparted enough thermal energy into the Si surface to allow the SiCl layer to escape the surface [Fig. 1(a)(iii)]. Nanosecond pulse duration was used for chlorine dissociation due to high pulse energies and therefore high Cl₂ dissociation rates that can be achieved easily. 266 nm wavelength was chosen due to laser availability, however 330-355 nm dissociation pulses are expected to achieve maximal coupling to the Cl2 gas. We used picosecond etching pulses due to their ability to rapidly heat a surface with minimal thermal penetration, and 355 nm was chosen due to availability combined with its very thin optical absorption depth. This overall maximizes the spatial confinement of the etching. Further description of the LaCVD system layout is included as supplementary information, see supplementary material.

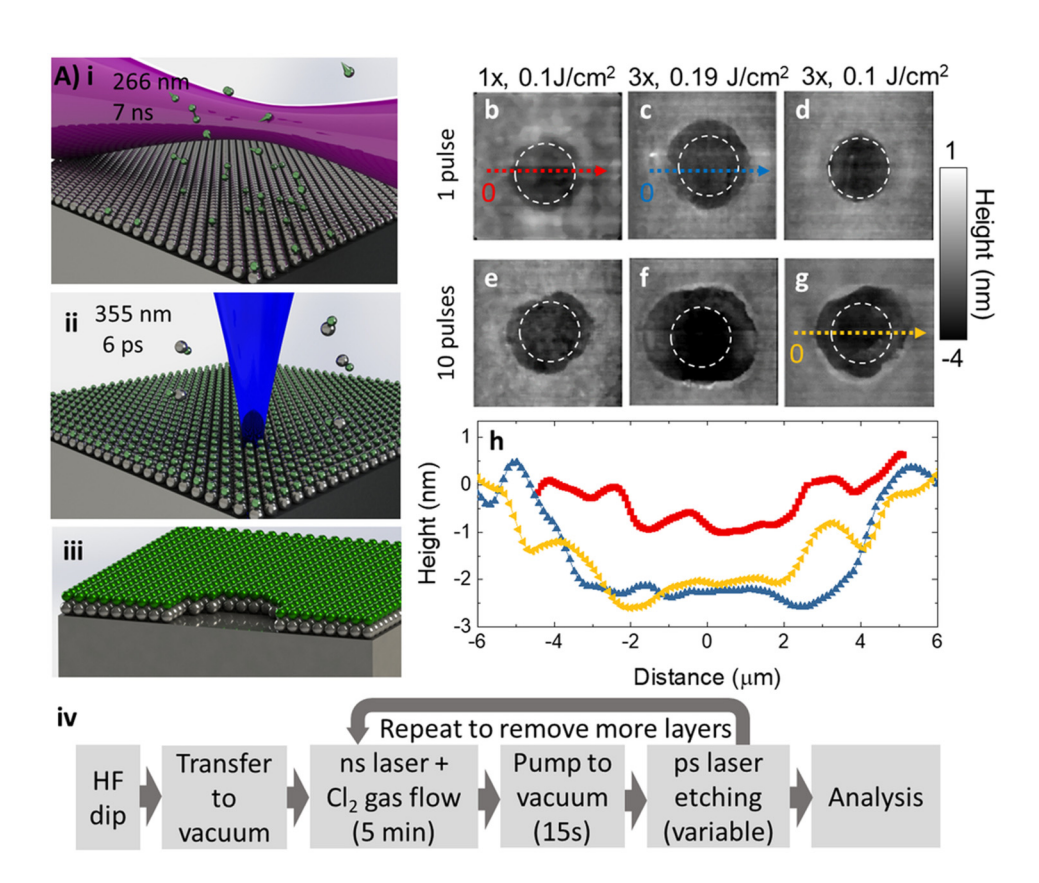


FIG. 1. (a) Diagram of pulsed laser induced atomic layer etching process: Nanosecond laser chlorination, 266 nm laser propagating parallel to the surface; (ii) Picosecond laser etching, with 355 nm laser directly irradiating silicon surface; (iii) etched result shown from a cross section in the middle of the etched region, with a single self-limited layer removed; (iv) process flowchart. The green and gray spheres in panel (a) indicate chlorine and silicon atoms, respectively. (b)-(g) AFM topography image of picosecond laser etching at varied parameters, edge length of images is $15 \mu m$; (h) AFM line traces of laser etch pits at the same parameters. Red squares -1x, 0.1 J/cm², 1 pulse, blue triangles - 3x, 0.19 J/cm², 1 pulse, yellow triangles - 3x, 0.1 J/cm², 10 pulses.

We performed three trials: picosecond laser etching without chlorination, with one cycle of chlorination and etching, and three cycles of chlorination and etching. We attempted the picosecond laser etching without chlorination as a control to ensure the selflimited etching was due to the SiCl surface layer chemical bonding. Each of these three conditions was repeated for both a single picosecond laser etching pulse and 10 pulses. The picosecond laser heating also created a very thin layer of amorphized silicon, which was not measurable via Raman spectroscopy. The absorption depth of silicon at this wavelength is only 10 nm, before considering the effect of two photon absorption associated with the photon flux carried by the picosecond laser pulse. From previous investigation of picosecond UV-laser irradiation of silicon at similar fluence and pulse duration, the pulsed irradiation in our experiment is expected to create a molten silicon layer approximately 40 nm deep. Upon freezing, this layer becomes fully amorphized due to the fast conductive heat transfer loss to the underlying solid silicon.²⁶ The amorphization produced a slightly more reflective region in the optical microscope image where the pulse irradiated. This amorphized layer was then re-crystallized by CW laser annealing with a 532 nm laser (Sprout) at 14 MW/cm², scanning a 3 μm beam spot at $10 \,\mu\text{m/s}$ with a lateral step of $3 \,\mu\text{m}$ as well. This eliminated any evidence of amorphization, and the surface remained planar to within measurement error. Finally, we analyzed the surface topography by an AFM instrument (VistaScope by Molecular Vista).

We used a numerical simulation to model the temperature near the CW laser beam spot and assessed that solid state annealing is feasible at the fluences used here. It is known from previous investigation that rapid solid state crystallization of amorphous silicon films can be observed at 1053 K.²⁷ Because the thermal conductivity of silicon is highly nonlinear in the temperature regime from 300 K and 1053 K, linear solutions to the conduction equation cannot be employed, so numerical simulation was necessary. We modeled the temperature fields to find what region of the material reached temperatures above the annealing temperature. This was done with the COMSOL heat transfer simulation software, and further details of the simulation are given as supplementary information, see supplementary material. We found that the maximum radius at which a minimum temperature of 1053 K was reached was $2.05 \mu m$, or a diameter of $4.1 \,\mu\text{m}$. The lateral step size of the annealing scan was $3 \mu m$, smaller than the annealed diameter, so the entire scanned region reached the required temperature. Therefore, we confirmed the CW irradiation performed can generate temperatures that induce solid state annealing. If more precise temperature measurements are required for future process development, known methods of in-situ optical temperature measurement may be employed.²

For the case of picosecond pulses without prior chlorination, there was no measurable change in substrate topography after re-crystallization. Therefore, etching was only possible using a prior chlorination step, whereas direct etching solely by desorption/ablation without a chlorination process cannot induce etching. Figures 1(b)–1(g) display the AFM images of the etching for 6 combinations of parameters, accompanied by Table I, displaying the etch depth for the same parameters. From the table, we can see that the etching was consistently ~0.85 nm in depth per cycle (EPC) regardless of the number of picosecond laser pulses or fluence. This sharp self-limiting behavior and etch depth is consistent with ALEt that

TABLE I. Depth values of picosecond laser etching at varied parameters.

Depth chart (nm)	1 pulse	10 pulses
3x, 0.1 J/cm ²	2.281	2.839
3x, 0.19 J/cm ²	2.468	2.827
1x, 0.1 J/cm ²	.854	.880

has been observed previously using the ${\rm Ar}^+$ bombardment approach. This EPC deviation from that of a single atomic layer is theorized to be due to energetic Cl species penetration through the surface, which has been observed in molecular dynamic simulation and further agrees with the EPC observed here. The images suggest a quite flat bottom of the etching pit despite the Gaussian distribution of the picosecond laser beam. The depth profiles in Fig. 1(h) also show a relatively flat crater bottom to within the measurement root mean square error of 0.37 nm.

We additionally performed the etching process for partially overlapping laser focal spots, with results shown in Fig. 2. We irradiated one spot once with the picosecond laser, labeled II, and we irradiated the second spot twice, labeled III, with an overlapping region in the middle, labeled IV. Region I has not been irradiated. This created separate regions that had been processed between 0 and 3 times, with each subsequent exposure removing a single 0.85 nm layer. Figure 2(b) shows the equal spacing between each processing level and the flat bottom of the etch pits. This demonstration illustrates the sharp and repeatable etching thresholds,

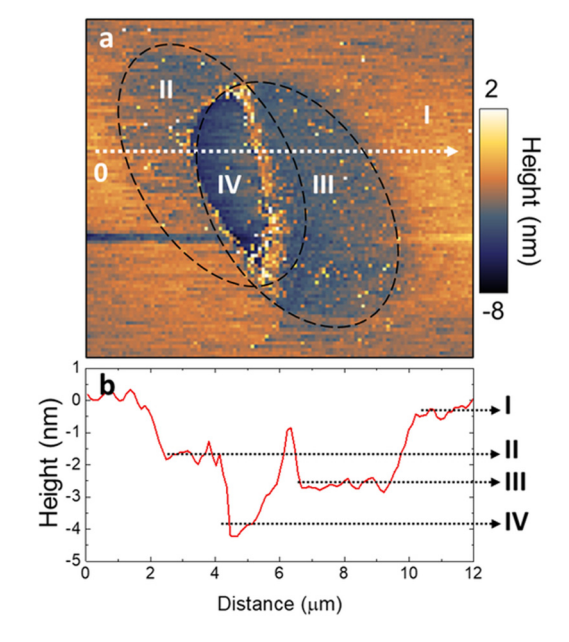


FIG. 2. (a) AFM image of two overlapping etching pits that were etched at 0.19 J/cm² with 10 picosecond pulses each. Region I is unmodified, region II receives 1 cycle, region III receives 2 cycles, and region IV is the overlap which receives 3 cycles. (b) AFM profile plot corresponding to the region indicated by the dotted white line. The dotted black line indicates the outline of each ps laser spot.

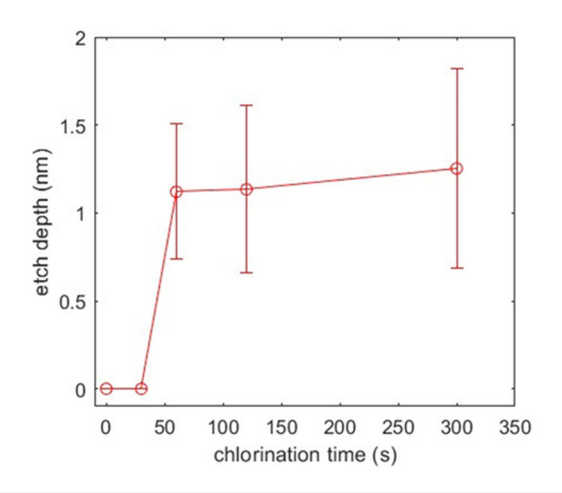


FIG. 3. Etch depth as a function of chlorination time measured by AFM. Error bars indicate rms error of AFM measurement.

which can be applied to both etched and unetched surfaces concurrently.

We additionally performed etching at various chlorination durations from 0–5 min to measure the time necessary to saturate the silicon surface with chlorine sufficiently to perform the etching. We again used AFM to determine if any etching was present, and if so, the depth of the etching. The results are plotted in Fig. 3. At chlorination durations less than 30 s, no etching was observed, however for 60 s and greater chlorination times, the etch depth was approximately constant, and in agreement with other measurements from Figs. 1 and 2. We therefore observed clear self-limiting

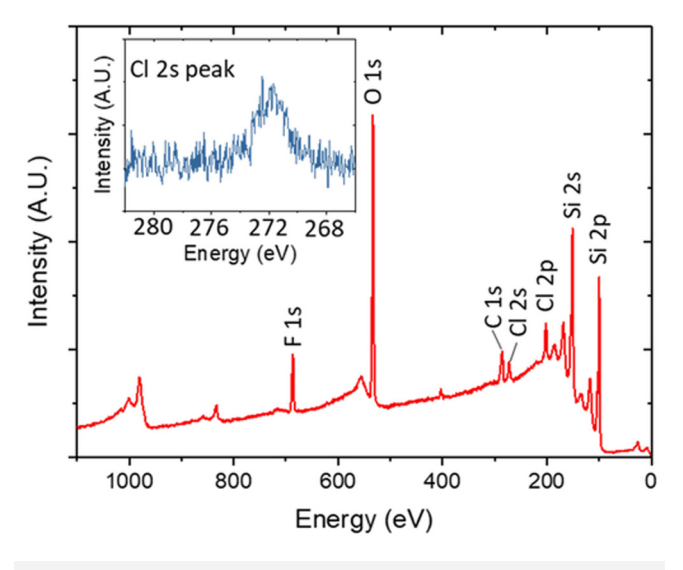


FIG. 4. XPS data for the chlorinated silicon sample with peaks labeled. Inset is high resolution XPS data for the Cl2s peak. Chlorine peaks are clearly visible, with incidental carbon contamination and residual fluorine from HF dip.

behavior of the etching with respect to the chlorination time, pulse number and pulse fluence.

To confirm the presence of chlorine on the surface of the silicon chip, we performed XPS after the chlorination. A survey in the range of 0–1100 eV of binding energy is displayed in Fig. 4. From the peaks, we observed silicon and oxygen in highest concentration, as well as chlorine, as expected. Additionally, we observed some carbon from incidental contamination, and fluorine, residual from the HF dip. The inset displays the Cl2s peak, which is clearly observed in high resolution to have a normal distribution and peak indicative of the presence of chlorine at a binding energy of 272 eV. This sample was handled with a high degree of cleanliness, and this chlorine can only be due to the chlorination process.

III. CONCLUSIONS

In summary, we demonstrated ALEt of silicon using chlorination and an all-optical method of Cl2 gas dissociation, etching, and annealing. We used pulsed nanosecond laser radiation to dissociate the Cl₂ gas which adsorbed to the surface of the silicon, then irradiated a picosecond pulsed laser to desorb the SiCl layer. We characterized the dependence of the etch depth on chlorination time, laser fluence, and number of etch pulses, and found sharp selflimiting behavior in each variable. Using pulsed lasers to perform these aspects of the processing in a digital manner should yield significant benefits both in process control, processing time and cost of production. We report the chlorination time at 60 s, or 600 individual pulses at 10 Hz, however the use of higher repetition rate pulsed lasers would decrease the processing time. Additionally, the absorption cross section of Cl2 gas can be increased by nearly a factor of 10 by irradiating closer to the peak absorption wavelength of 330 nm, or even at the more accessible laser source at 355 nm (the third harmonic of an Nd:YAG source). Finally, increasing the concentration of Cl2 gas should provide a significant saturation time decrease. Although the saturation time dependence is complex, 100X change in concentration of Cl2 should speed up the process significantly. Taken together, future design should be able to reduce the time until saturated chlorination to below the 1 s timeframe given by plasma chlorination. Additionally, scaling the power of the picosecond processing beam with its spot size should give laser etching times far faster than Argon ion bombardment. Current off the shelf high-power lasers can produce picosecond pulses at high repetition rates with average power on the order of 100 Watts. Assuming the minimum etching dose used in this study of 1 pulse at 0.1 J/cm², the total energy dose required for a 300 mm wafer is 70.7 J, which a 100 W laser could provide in 0.71 s. For direct maskless laser writing, a galvanometric scanner may be a convenient implementation. Polygonal scanning³⁰ has been developed to scan at high speeds that allow for efficient irradiation even for MHz repetition rates. Incorporation of a photomask could enable direct laser writing with a spatially modulated high power picosecond beam. This leaves only the time taken to transition from 200 Torr of Cl₂ gas to moderate vacuum via mechanical pump, and the vacuum requirement for laser etching is much lower than required for ion bombardment, so this requirement also favors the current laser mediated process. One key area for future work is to demonstrate anisotropic etching via laser assisted ALEt,



which is a key benefit of industrial application of ALEt. While thermal desorption of SiCl with heating times in the range 8–20 s is known to produce isotropic etching, ^{1,2} our method produces peak temperatures at picosecond timescales, which can be expected to induce significantly different desorption dynamics. Further, these temperatures can be highly spatially confined when delivered by the laser. Optimal anisotropic etching may involve different selection of laser pulse duration and wavelength to precisely confine the heated region to etch anisotropically.

ACKNOWLEDGMENTS

M.E. and Y.R. equally contributed to this work. Financial support awarded to the University of California, Berkeley, by the National Science Foundation through Grant CMMI-2024391 is gratefully acknowledged. Part of this work by Y.R. was performed under the auspices of the U.S. Department of Energy by Lawrence Livermore National Laboratory under Contract DE-AC52-07NA27344. The chlorination experiments were conducted at the Laser Assisted Chemical Vapor Deposition (LACVD) apparatus at the UC Berkeley Marvell Nanofabrication Laboratory.

AUTHOR DECLARATIONS

Conflict of Interests

The authors have no conflicts to disclose.

Author Contributions

Matthew Eliceiri: Conceptualization (lead); Data curation (lead); Formal analysis (lead); Investigation (lead); Methodology (equal); Validation (equal); Visualization (lead); Writing – original draft (lead); Writing – review & editing (equal). Yoonsoo Rho: Conceptualization (equal); Investigation (equal); Methodology (equal); Validation (equal); Visualization (equal); Writing – original draft (equal); Writing – review & editing (equal). Runxuan Li: Data curation (supporting); Formal analysis (supporting); Investigation (supporting); Software (supporting); Validation (supporting). Costas Grigoropoulos: Conceptualization (equal); Funding acquisition (lead); Investigation (supporting); Methodology (equal); Project administration (lead); Resources (lead); Supervision (lead); Writing – review & editing (equal).

DATA AVAILABILITY

The authors will make available all data presented in the paper upon reasonable request.

REFERENCES

- ¹ K. J. Kanarik, T. Lill, E. A. Hudson, S. Sriraman, S. Tan, J. Marks, V. Vahedi, and R. A. Gottscho, J. Vac. Sci. Technol. A 33, 020802 (2015).
- ²S. Imai, T. Haga, O. Matsuzaki, T. Hattori, and M. Matsumura, Jpn. J. Appl. Phys. 34, 5049 (1995).
- ³T. Matsuura, J. Murota, Y. Sawada, and T. Ohmi, Appl. Phys. Lett. **63**, 2803 (1993).
- ⁴K. J. Kanarik, S. Tan, A. Eppler, J. Marks, and R. A. Gottscho, Solid State Technol. **56**, 14 (2013).
- ⁵C. K. Oh, S. D. Park, H. C. Lee, J. W. Bae, and G. Y. Yeom, Electrochem. Solid-State Lett. 10, H94 (2007).
- ⁶K. K. Ko and S. W. Pang, J. Vac. Sci. Technol. B 11, 2275 (1993).
- ⁷H. Sakaue, S. Iseda, K. Asami, J. Yamamoto, M. Hirose, and Y. Horiike, Jpn. J. Appl. Phys. 29, 2648 (1990).
- 8S. D. Athavale and D. J. Economou, J. Vac. Sci. Technol. B 14, 3702 (1996).
- ⁹G. S. Oehrlein, D. Metzler, and C. Li, ECS J. Solid State Sci. Technol. 4, N5041 (2015)
- ¹⁰B.-J. Kim, S. Chung, and S. M. Cho, Appl. Surf. Sci. **187**, 124 (2002).
- ¹¹S.-D. Park, K.-S. Min, B.-Y. Yoon, D.-H. Lee, and G.-Y. Yeom, Jpn. J. Appl. Phys. **44**, 389 (2005).
- ¹²S. D. Park, D. H. Lee, and G. Y. Yeom, Electrochem. Solid-State Lett. **8**, C106 (2005)
- ¹³D. J. Economou, J. Phys. D: Appl. Phys. **41**, 024001 (2008).
- ¹⁴S. D. Park, C. K. Oh, D. H. Lee, and G. Y. Yeom, Electrochem. Solid-State Lett. 8, C177 (2005).
- ¹⁵H. J. Yun, T. H. Kim, C. B. Shin, C.-K. Kim, J.-H. Min, and S. H. Moon, Korean J. Chem. Eng. 24, 670 (2007).
- ¹⁶A. Agarwal and M. J. Kushner, J. Vac. Sci. Technol. A 27, 37 (2009).
- ¹⁷K. Suzue, T. Matsuura, J. Murota, Y. Sawada, and T. Ohmi, Appl. Surf. Sci. 82–83, 422 (1994).
- 18S. D. Athavale and D. J. Economou, J. Vac. Sci. Technol. A 13, 966 (1995).
- 19 J. R. Vella, D. Humbird, and D. B. Graves, J. Vac. Sci. Technol. A 40, 023205 (2022).
- 20 Y. Rho et al., Nat. Electron. 5, 505 (2022).
- ²¹B. Y. Han, C. Y. Cha, and J. H. Weaver, J. Vac. Sci. Technol. A **16**, 490 (1998).
- ²²P. A. Maki and D. J. Ehrlich, Appl. Phys. Lett. 55, 91 (1989).
- 23T. Baller, D. J. Oostra, A. E. de Vries, and G. N. A. van Veen, J. Appl. Phys. 60, 2321 (1986).
- ²⁴H. Okano, Y. Horiike, and M. Sekine, Jpn. J. Appl. Phys. 24, 68 (1985).
- ²⁵R. Kullmer and D. Bäuerle, Appl. Phys. A **43**, 227 (1987).
- ²⁶P. H. Bucksbaum and J. Bokor, Phys. Rev. Lett. **53**, 182 (1984).
- ²⁷L. Haji, P. Joubert, J. Stoemenos, and N. A. Economou, J. Appl. Phys. 75, 3944 (1994).
- ²⁸M. Hatano, S. Moon, M. Lee, K. Suzuki, and C. P. Grigoropoulos, J. Appl. Phys. 87, 36 (2000).
- ²⁹P. Brichon, E. Despiau-Pujo, and O. Joubert, J. Vac. Sci. Technol. A 32, 021301 (2014)
- ³⁰U. Loeschner, J. Schille, A. Streek, T. Knebel, L. Hartwig, R. Hillmann, and C. Endisch, J. Laser Appl. 27, S29303 (2015).